

COMPARISON OF INDUCTOR MODELS USED IN ANALYSIS OF THE BUCK AND BOOST CONVERTERS

Krzysztof Górecki, Witold J. Stepowicz

Gdynia Maritime University, Department of Marine Electronics, Poland

Key words: dc-dc converters, SPICE, inductor models

Abstract: The inductive devices with the ferromagnetic core are widely used in many electronic circuits, for example in the buck and boost converters, to store magnetic energy. They should be treated as nonlinear devices, and the nonlinearity of their characteristics arises from the dependence of inductance on current. In the paper the influence of the nonlinear and linear inductor models on some selected characteristics of the above-mentioned converters is compared. As a tool to compute these characteristics SPICE was used.

Primerjava modelov induktivnosti uporabljenih pri analizi konverterjev

Ključne besede: DC-DC konverterji, SPICE, modeli induktivnih komponent

Izveček: Induktivne komponente na feromagnetnih jedrih pogosto uporabljamo v mnogih elektronskih vezjih, npr. v DC-DC konverterjih, za shranjevanje magnetne energije. Potrebno jih je obravnavati kot nelinearne elemente, saj njihova nelinearna karakteristika izhaja iz tokovne odvisnosti induktivnosti. V prispevku primerjamo vpliv linearnih in nelinearnih modelov induktivnosti na delovanje konverterjev. Pri analizi smo uporabili program SPICE.

1. Introduction

In the dc-dc converters, which are the basic part of switched voltage regulators, the inductors with ferromagnetic core are used to store magnetic energy /1, 2/. These inductors should be characterized by the high value of the permeability and the high value of the saturation induction. The inductor with the ferromagnetic core is a nonlinear device, what results from the dependence of its inductance on current. The inductance decreases strongly with current, when the operation point of the core is moved to the saturation range of the magnetic induction, and it can cause the limitation of the allowable output current (or the load resistance) of a voltage regulator.

To design the dc-dc converters and other electronic circuits computer programs are used, and nowadays SPICE belongs to the most popular computer tools /3, 4/. In SPICE the models of many electronic devices are built-in, and to obtain reliable results of analysis, they should be simple, accurate and with credible values of their parameters. As far as inductors are concerned their linear and nonlinear SPICE models are described in /5/.

In Sec. 2 the nonlinear model of inductor is presented, and the basic characteristics and parameters of the selected inductor under consideration are given. As the main purpose of this paper is to show the influence of the nonlinear model of the inductor on some important characteristics of the typical buck and boost converters, therefore the basic characteristics of these circuits with the linear and nonlinear inductor models taken into account were computed to this end, and they are shown and discussed

in Sec. 3. By comparing the characteristics obtained on the nonlinear model with the characteristics obtained on the linear one some remarks concerning the usefulness of the nonlinear model in the analysis of the converters are given in Sec. 4.

2. Nonlinear model of inductor

In SPICE two nonlinear models of the inductors with the ferromagnetic core are attainable: Jiles-Atherton model (JA model) /6/ and SPICE Plus model. On the models the hysteresis curve B(H) causing this nonlinearity can be calculated. In the paper /9/ the results of the computations obtained on SPICE, showing the sensitivity of the nonlinear dependence L(i) on the parameters of the JA model, are given.

In SPICE the isothermal analysis, which is the analysis at any constant ambient temperature, is possible, without taking into account the temperature rise caused by energy losses (the self-heating phenomenon) in the inductor. The electrothermal model of the inductor allowing the electrothermal analysis with the self-heating taken into consideration is proposed in /7/.

The essential dependences of the JA model needed to compute the curve B(H) are as follows

$$B = \mu_0 \cdot (H + M) \quad (1)$$

$$M_{an} = \frac{MS \cdot H}{H + A} \quad (2)$$

$$\frac{dM}{dH} = \frac{1}{1+C} \cdot \frac{M_{an} - M}{K} + \frac{C}{1+C} \cdot \frac{dM_{an}}{dH} \quad (3)$$

where: B – magnetic induction, μ_0 – permeability of vacuum, H – magnetic field, M – magnetisation, M_{an} – initial magnetisation, and the parameters of the model are: MS – saturation magnetisation, A – thermal energy parameter, K – domain anisotropy parameter, C – domain flexing parameter. On the computed dependence $B(H)$ the incremental permeability μ can be obtained, which is needed to calculate the inductance L .

To compute the dependence $L(i)$, at first the magnetic field H is calculated at any assumed current i according to

$$H = \frac{i \cdot z}{l} \quad (4)$$

where: z – number of coils, l – length of the magnetic path (core model parameter $PATH$). When H is given, the hysteresis curve $B(H)$ can be computed on the basis of the formulae (1-3), then the incremental permeability μ at the assumed current can be calculated, and the inductance L is given as follows /8/

$$L = \frac{z^2 \cdot \mu_0 \cdot S}{l} \cdot \frac{dB}{dH} \quad (5)$$

where S – the cross-section of the core (core model parameter $AREA$).

In the computations presented below the following values of the parameters of the considered core were assumed /9/: $MS = 412.2$ A/m, $A = 44.82$ A/m, $K = 25.74$ A/m, $C = 0.411$ A/m (taken from SPICE library $MAGNETIC.LIB$ for $K528T500_3C8$ core). The magnetic path was $l = 3.84$ cm, the coil number $z = 10$ and the cross-section area of the core $S = 0.63$ cm². The hysteresis curve at the frequency $f = 10$ kHz and the dependence $L(i)$ of the inductor computed with the above given parameters values are shown in Fig. 1a, b, respectively.

As seen from Fig. 1a, the saturation induction of the considered core amounts about 430 mT (after converting units of measure, as in SPICE the magnetic field is denominated in oersted (Oe) and the magnetic induction in gauss (Ga)). The derivative dB/dH attains its maximum value at the inductor current equal to about 100 mA.

As seen from Fig. 1b, for the inductor under consideration the inductance L decreases with current increase from $L = 590$ μ H in low and medium current range to $L = 35$ μ H at 1 A, what corresponds to the start of the saturation range of the $B(H)$ curve, and next up to $L = 0.2$ μ H at the high current equal to about 100 A, when the operation point is placed in the deep saturation range of the dependence $B(H)$.

3. Influence of inductor models on the characteristics of converters

The computations of the selected characteristics were carried out for the buck (Fig. 2a) and boost (Fig. 2b) converters. The following basic characteristics were considered: the dependence of the output voltage V_o and the

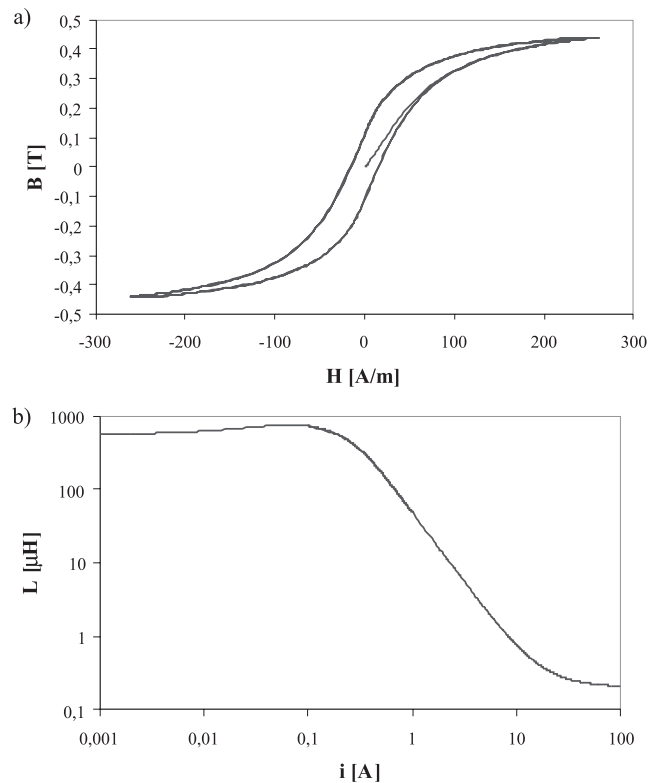


Fig. 1. The hysteresis curve $B(H)$ of the core (a), and the dependence of the inductance on the inductor current (b)

efficiency η on the load resistance R_o , on the duty factor d and on the input voltage V_i . Additionally, the dependence of the peak-to-peak output voltage (ripples) V_{pp} on the load resistance was computed as well. These dependences were computed with the nonlinear model of the inductance L , which characteristics (Fig. 1) and parameters values are given in Sec. 2, and, for comparison, with the linear model at three values of the inductance L equal to 590 μ H (corresponding to the low and medium current range), with 35 μ H (corresponding to $i = 1$ A) and with 0.2 μ H (corresponding to $i = 100$ A). The computations were carried out by SPICE at the ambient temperature $T = 300$ K. In these computations the SPICE built-in models of the diode and MOS transistor were used with their parameters values taken from library $EVAL.LIB$ for diode 1N4148 and transistor IRF150. For two considered converters $R2 = 10$ Ω and $C = 470$ μ F were assumed. The voltage source $V2$ supplies the trapezoidal pulse run with the low and high levels of the transistor input voltage v_{GS} equal to 0 and 10 V, respectively; the period of this run is equal 10 μ s (Fig. 2).

3.1 The buck converter

For the buck converter (Fig. 2a), the dependences $V_o(R_o)$ and $\eta(R_o)$ with the duty factor $d = 0.5$ and the input voltage $V_i = -20$ V, next the dependences $V_o(d)$ and $\eta(d)$ with $R_o = 100$ Ω and $V_i = -20$ V were computed, while the dependences $V_o(V_i)$ and $\eta(V_i)$ with $d = 0.5$ and $R_o = 0.5$ Ω , respectively. These all characteristics were calculated at three

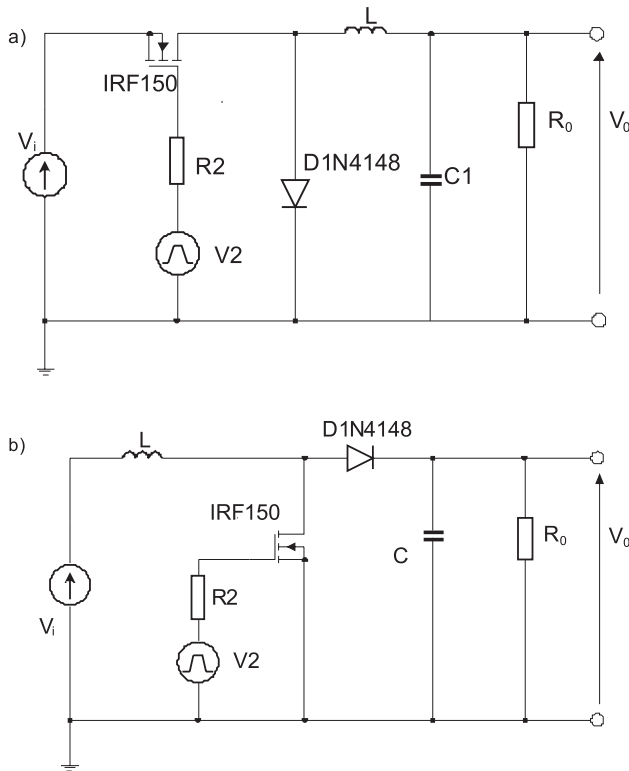


Fig. 2. The schemes of the buck (a), and boost (b) converters

values of the linear inductance taken from the different current ranges of the dependence $L(i)$ and with the nonlinear model of $L(i)$ described in Sec. 2.

In Figs 3a, b the characteristics $V_o(R_o)$, and $\eta(R_o)$ are shown, respectively. As seen from Fig. 3a, at low load resistances (high currents), when the core saturates, the dependences $V_o(R_o)$ do not differ considerably for the nonlinear model, the linear model with at $L = 590 \mu\text{H}$ and at $L = 35 \mu\text{H}$, while at high resistances (low currents), without core saturation, only the results obtained on the nonlinear model of $L(i)$ and on the linear model at $L = 590 \mu\text{H}$ are similar to each other. In the whole resistance range the characteristic with $L = 0.2 \mu\text{H}$ differs from other characteristics considerably.

As it results from computations (Fig. 3a), the converter operates in the current continuous mode (CCM) at $R_o < 200 \Omega$ as the nonlinear model $L(i)$ was used, while on the linear model the lower values of this resistance are obtained: $R_o = 10 \Omega$ at $L = 35 \mu\text{H}$ and $R_o = 0.2 \Omega$ at $L = 0.2 \mu\text{H}$, what, in turn, leads to high differences in the computed values of the output voltage obtained on the considered models in the discontinuous current mode (DCM) especially.

From Fig. 3b it results that the computed efficiency η obtained on the nonlinear model of $L(i)$ is lower than η resulting from the linear model in the whole range of the assumed values of R_o . These divergences result from the energy losses in the core taken into account in the nonlin-

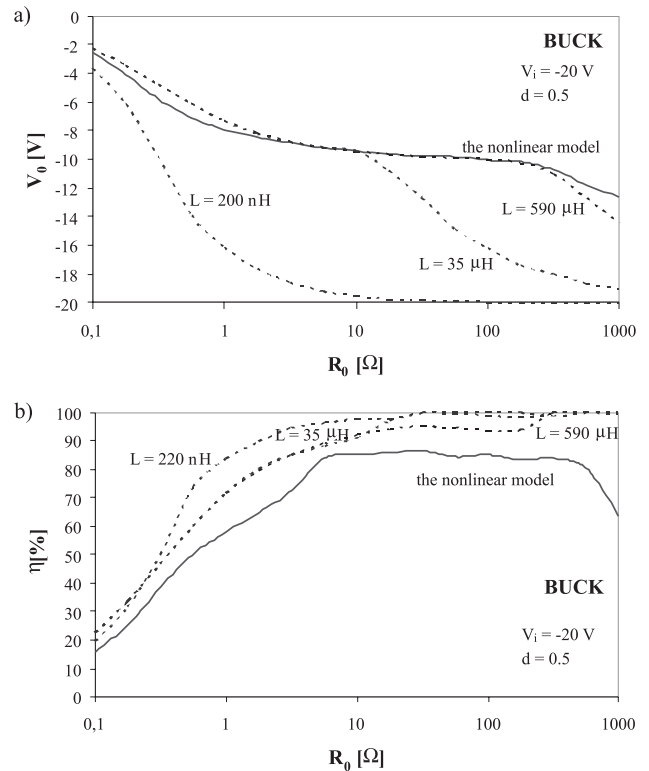


Fig. 3. The dependences of the output voltage (a), and the efficiency (b) on the load resistance for the buck converter

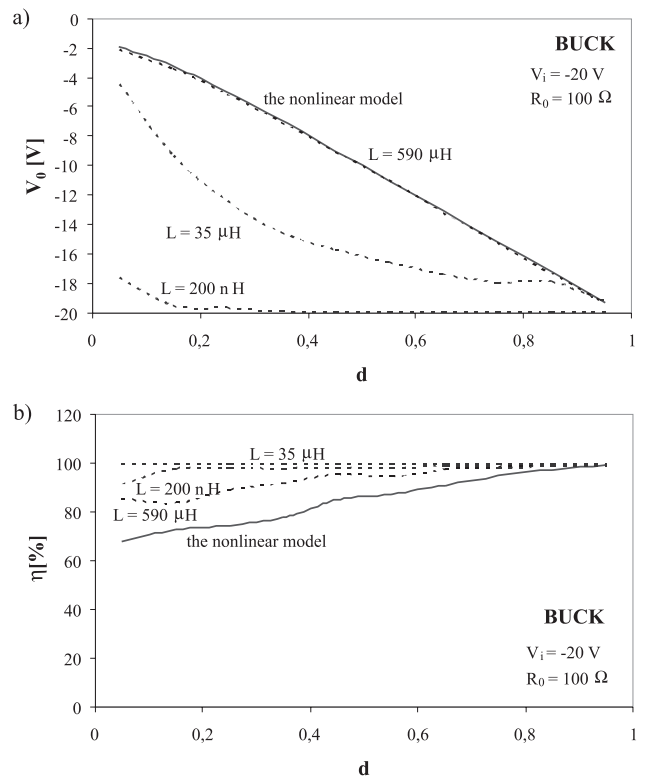


Fig. 4. The dependence of the output voltage (a), and the efficiency (b) on the duty factor for the buck converter

ear model. With the decreasing inductance the efficiency increases.

In Figs 4a, b the characteristics $V_o(d)$ and $\eta(d)$ are shown, and as seen from Figs 4a the essential difference is observed between the dependence $V_o(d)$ with $L = 200$ nH and $L = 35$ μ H in relation to other curves. As stated before, at $R_o = 100$ Ω the core does not saturate.

From Fig. 4b it results that, as before, the computed efficiency η obtained on the nonlinear model is lower than η resulting from linear model in the whole range of the assumed duty factor d practically, what is caused by the energy losses taken into account in the nonlinear model.

In Figs 5a, b the characteristics $V_o(V_i)$ and $\eta(V_i)$ are shown with $R_o = 0.5$ Ω and $d = 0.5$ assumed. In this case these characteristics computed with $L = 35$ μ H and $L = 590$ μ H are practically identical. The voltage transfer characteristic with $L = 200$ nH (Fig. 5a) differs from the curves with other values of the inductance considerably. The efficiency η (Fig. 5b) obtained on the nonlinear model is lower about 20% than η obtained on the linear model.

The dependence of the ripples of the output voltage on the load resistance $V_{pp}(R_o)$ is shown in Fig. 6. As it could be expected [1], the ripples decrease with the increase of the inductance. The highest ripples are at low values of R_o – for the nonlinear model they amount above 100 mV, and at $L = 590$ μ H they amount about 100 μ V.

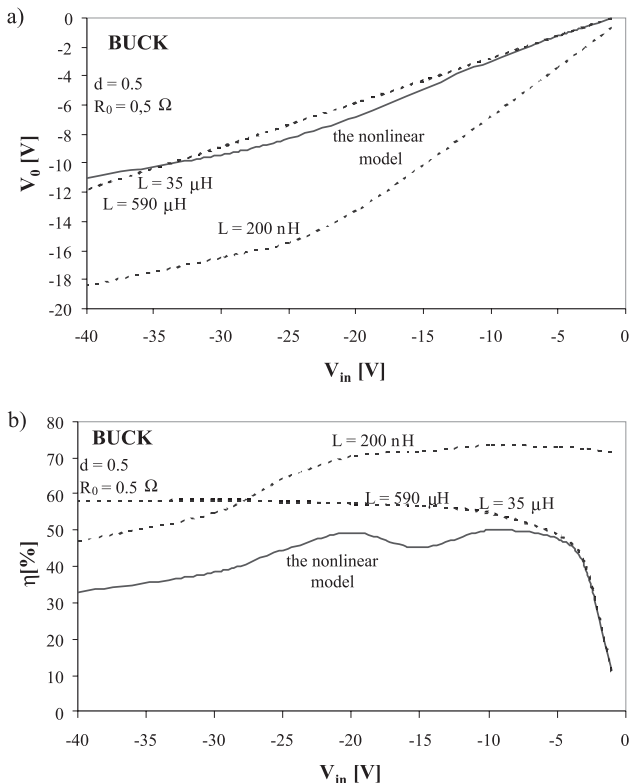


Fig. 5. The dependence of the output voltage (a), and the efficiency (b) on the input voltage for the buck converter

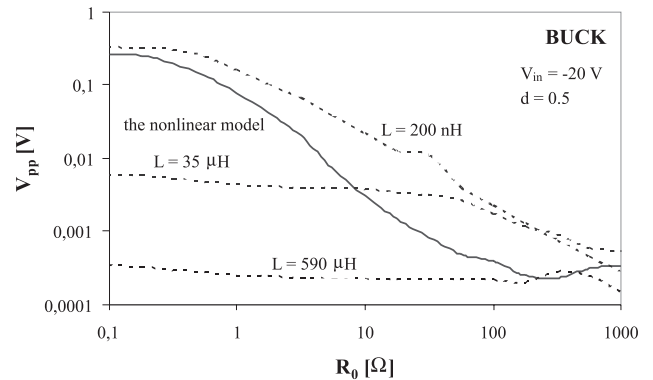


Fig. 6. The dependence of the ripples of the output voltage on the load resistance for the buck converter

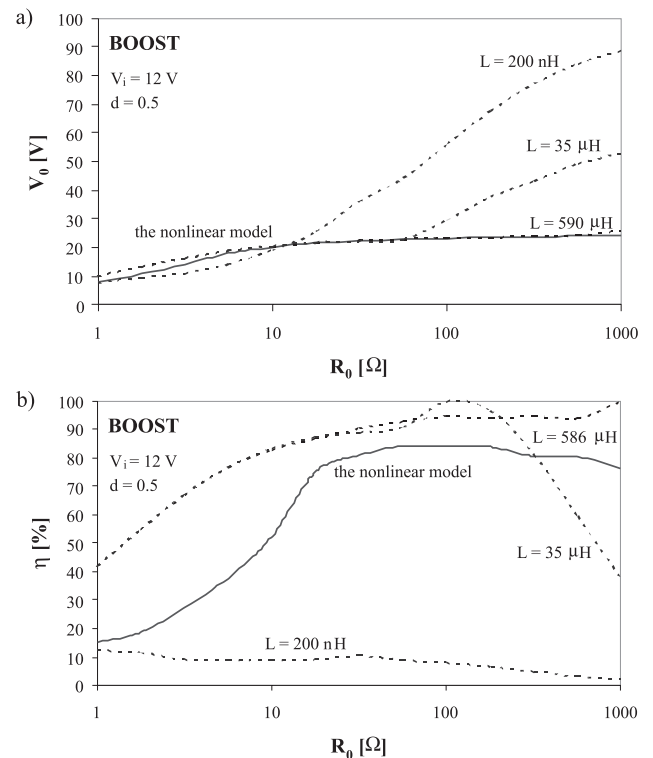


Fig. 7. The dependences of the output voltage (a), and the efficiency (b) on the load resistance for the boost converter

3.2 The boost converter

For the boost converter (Fig. 2b) the characteristics $V_o(R_o)$ and $\eta(R_o)$ were computed with $d = 0.5$ and $V_i = 12$ V, next $V_o(d)$ and $\eta(d)$ with $R_o = 3$ Ω and $V_i = 12$ V, and $V_o(V_i)$ and $\eta(V_i)$ with $d = 0.5$ and $R_o = 3$ Ω .

In Figs 7a, b the characteristics $V_o(R_o)$ and $\eta(R_o)$ are shown. As seen from Fig. 7a, the noticeable differences between the curves for all inductances assumed are at higher values of the load resistance, when the core does not saturate. At $L = 590$ μ H and at the nonlinear model of the inductance the converter operates in CCM in the whole considered range of the load resistance. At the lower induct-

ances this mode is limited to $R_o = 70 \Omega$ (at $L = 35 \mu\text{H}$) and $R_o = 10 \Omega$ (at $L = 0.2 \mu\text{H}$).

The dependences $\eta(R_o)$ (Fig.7b) obtained at four inductances differ from each other considerably, at higher values of the load resistance especially, and the highest differences – even 80%, are visible at $L = 200 \text{ nH}$ with respect to other curves.

In Figs 8a, b the characteristics $V_o(d)$ and $\eta(d)$ are shown. As seen from Fig. 8a the differences between the obtained dependences $V_o(d)$ for the nonlinear model $L(i)$ and at $L = 0.2 \mu\text{H}$ are similar, while at $L = 35 \mu\text{H}$ and at $L = 590 \mu\text{H}$ the values of V_o are about 100 % higher than those for the nonlinear model.

From Fig. 8b it results that the dependences $\eta(d)$ obtained on the linear model of L differ from the dependence obtained on the nonlinear model considerably. For all considered inductor models the efficiency decrease with increasing duty factor.

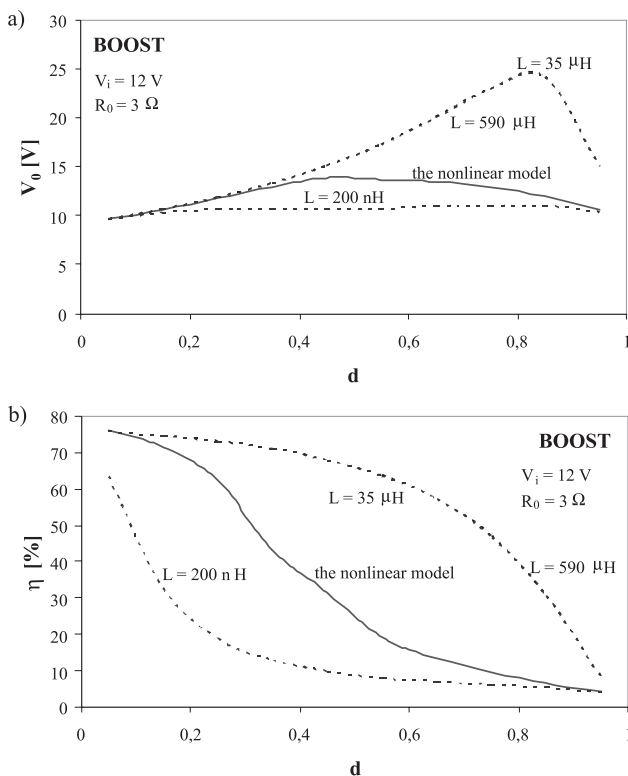


Fig. 8. The dependence of the output voltage (a), and the efficiency (b) on the duty factor for the boost converter

In Figs 9a, b the dependences $V_o(V_i)$ and $\eta(V_i)$ are shown. As seen from Fig. 9a, at low values of V_i there are no essential differences between the curves with the considered values of L , while at higher values of the input voltage they become visible.

As seen from Fig. 9b, the lowest values of the efficiency η are at $L = 200 \mu\text{H}$ - they amount about 10% only. For the nonlinear model the dependence $\eta(V_i)$ has the maximum at $V_i = 4 \text{ V}$.

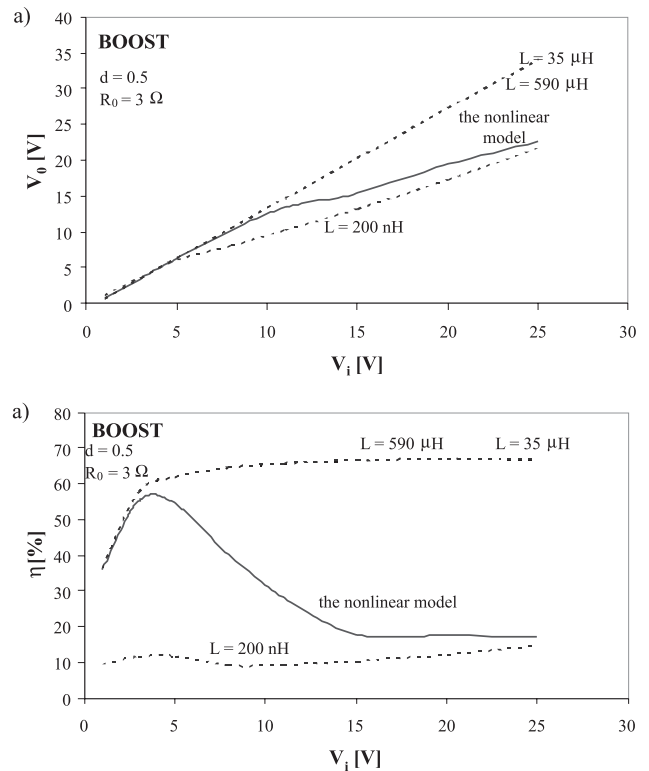


Fig. 9. The dependence of the output voltage (a), and the efficiency (b) on the input voltage of the boost converter

For the boost converter the dependence of the ripples of the output voltage on the load resistance $V_{pp}(R_o)$ is shown in Fig. 10. The ripples decrease with increasing the load resistance, and the increase of the inductance causes decreasing the ripples as well.

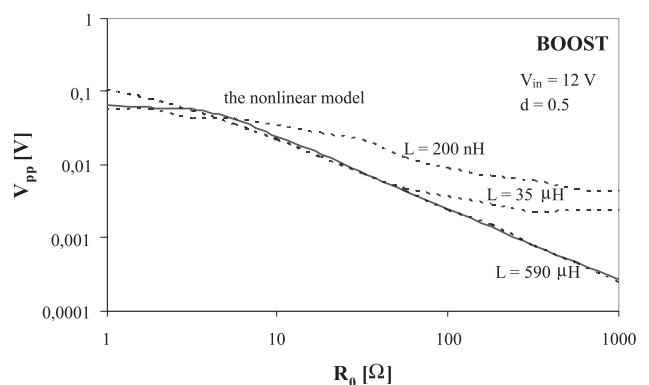


Fig. 10. The dependence of the ripples of the output voltage on the load resistance for the boost converter

4. Conclusions

In this paper the influence of the inductor model form on the selected characteristics of the buck and boost converters are discussed. The computations results are given for two models of inductance: the nonlinear JA model and

the linear one with the different values of L assumed. On these results one can estimate if the nonlinear model of the inductance is needed in the computer analysis of the converter to obtain reliable results. To this end the inductor current range should be evaluated in the first place.

If the core operates without saturation, then the divergences between the computations of the output voltage on the nonlinear model of L and on the linear one with the value of the inductance taken from the low current range are not essential. As the energy losses in the core are included in the nonlinear model of L, then the efficiency obtained on this model is typical lower than on the linear model, and the differences between these computations results of ζ can even amount some tens of percents.

It is worth-mentioning to compare the computation times of the characteristics presented in Sec. 3. Owing to the use of the linear model of the inductor the time needed to analyse any converter circuit is shortened up to 50%.

5. Acknowledgments

This work is supported by the Polish Ministry of Science and Higher Education in 2007-2008, as a research project No. N515 064 32/4331.

References

- /1/ R. Ericson, D. Maksimovic: Fundamentals of Power Electronics. Kluwer Academic Publisher, Norwell, 2001.
- /2/ Mohan N., Undeland T.M., Robbins W.P.: Power Electronics: Converters, Applications, and Design. John Wiley & Sons, New York, 1995.
- /3/ Vladimirescu A.: The SPICE Book. John Wiley & Sons, New York, 1994.
- /4/ Wilamowski B.M., Jaeger R.C.: Computerized Circuit Analysis Using SPICE Programs. McGraw-Hill, New York, 1997.
- /5/ Górecki K., Zarębski J.: Modelling of Inductors and Transformers in SPICE. Elektronika - konstrukcje, technologie, zastosowania, Not-Sigma, No. 1, 2004, pp. 40 – 43, in Polish.
- /6/ D.C. Jiles, D.L. Atherton: Theory of Ferromagnetic Hysteresis. Journal of Magnetism and Magnetic Materials, Vol. 61, 1986, p. 48.
- /7/ Górecki K.: SPICE-aided Modelling of Coils with the Ferrite Core with Selfheating Taken into Account. Kwartalnik Elektroniki i Telekomunikacji, No. 3, 2003, pp. 389 – 404, in Polish.
- /8/ W. Dąbrowski, J. Król, M. Soboń: Magnetic Materials for Ferromagnetic Ferroxyd Cores. Warszawa, Wydawnictwa Przemysłu Maszynowego "Wema", 1976, in Polish.
- /9/ Górecki K., Stepowicz W.J.: Influence of Inductor Models on the Characteristics of the Buck and Boost Converters. XXX International Conference on Fundamentals of Electrotechnics and Circuit Theory IC-SPETO 2007, Ustroń, 2007, p. 71.

*Dr. Krzysztof Górecki
Prof. Witold J. Stepowicz*

*Gdynia Maritime University
Department of Marine Electronics
Morska 83, 81-225 Gdynia, POLAND,
Tel. ++48 58 6901448, ++48 58 6901247,
fax ++48 58 6217353
E-mail: gorecki@am.gdynia.pl, wjs@am.gdynia.pl*

Prispelo (Arrived): 27.06.2007 Sprejeto (Accepted): 28.03.2008